ADVANCED ENERGY MATERIALS

Supporting Information

for *Adv. Energy Mater.,* DOI: 10.1002/aenm.201501659

Organic Salts as a Route to Energy Level Control in Low Bandgap, High Open-Circuit Voltage Organic and Transparent Solar Cells that Approach the Excitonic Voltage Limit

*John Suddard-Bangsund, Christopher J. Traverse, Margaret Young, Tyler J. Patrick, Yimu Zhao, and Richard R. Lunt**

WILEY-VCH

Supporting Information

Organic Salts as a Route to Energy Level Control in Low Bandgap, High Open-Circuit Voltage Organic and Transparent Solar Cells that Approach the Excitonic Voltage Limit

*John Suddard-Bangsund, Christopher J. Traverse, Margaret Young, Tyler Patrick, Yimu Zhao, Richard R. Lunt**

John Suddard-Bangsund, Christopher J. Traverse, Margaret Young, Tyler Patrick, Yimu Zhao, Prof. Richard R. Lunt
Department of Chemical Engineering and Materials Science, Michigan State University, East Lansing, MI, 48824 USA
Prof. Richard R. Lunt
Department of Physics and Astronomy, Michigan State University
East Lansing, MI, 48824 USA
*E-mail: (rlunt@msu.edu)

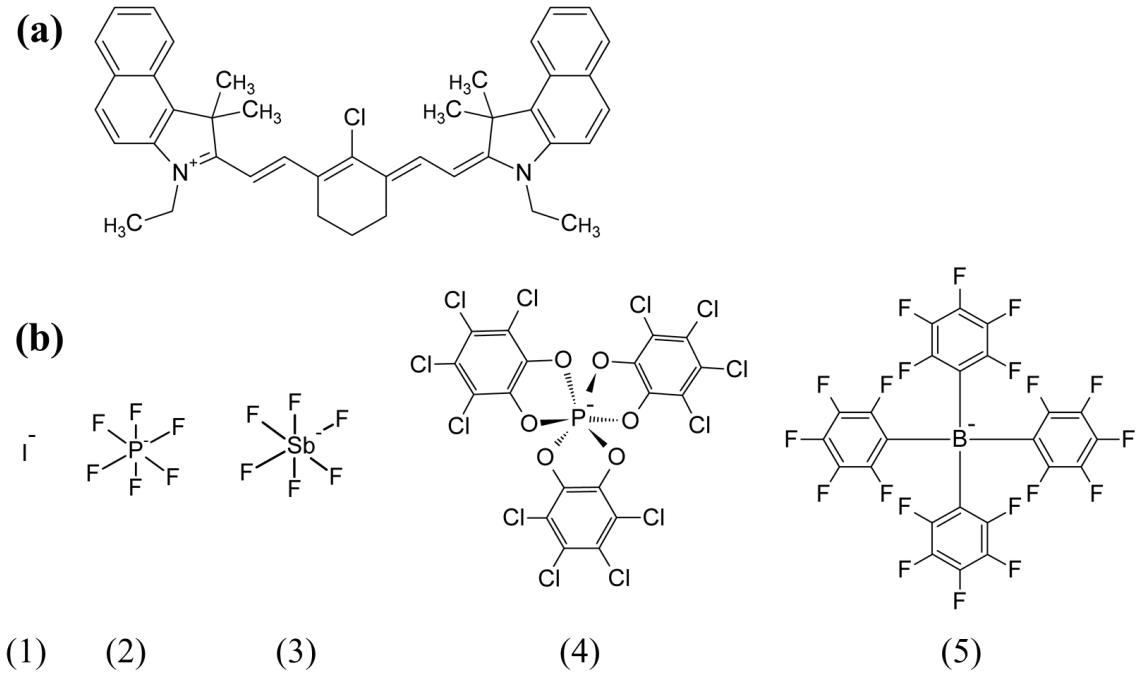

Figure S1. Molecular structures of (a) the Cy^+ cation, (b) the anions: (1) iodide, (2) hexafluorophosphate (PF_6^-), (3) hexafluoroantimonate (SbF_6^-), (4) Δ-TRISPHAT$^-$, and (5) TPFB$^-$.

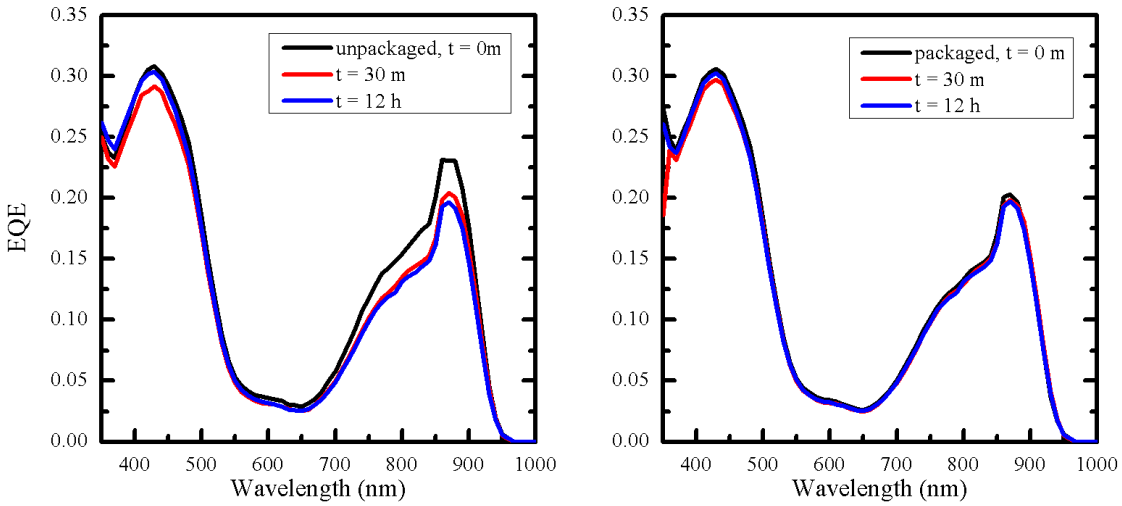

Figure S2. EQE lifetime testing of unpackaged (left) and packaged (right) devices. Unpackaged devices show up to an initial 10% drop after being exposed to air for 30 min but show no degradation for > 12hrs thereafter. In this manuscript, *J-V* data were collected prior to EQE data, and thus the reported EQE are typically lower bounds. Packaged devices show no clear drop off after 12 hours of exposure to air.

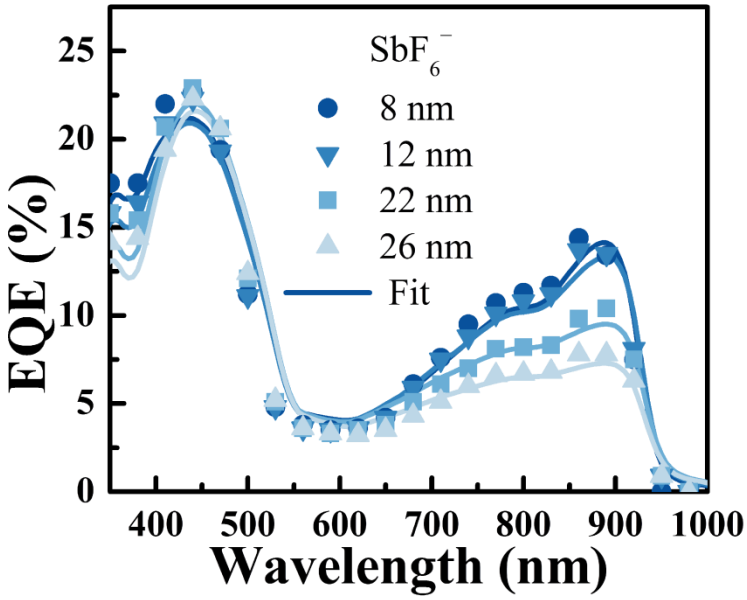

Figure S3. Measured (symbols) and fitted (solid lines) thickness dependent *EQE* spectra for $CySbF_6$. These spectra were fit for L_D, the results of which can be found in Table 3 and Figure 6(b).

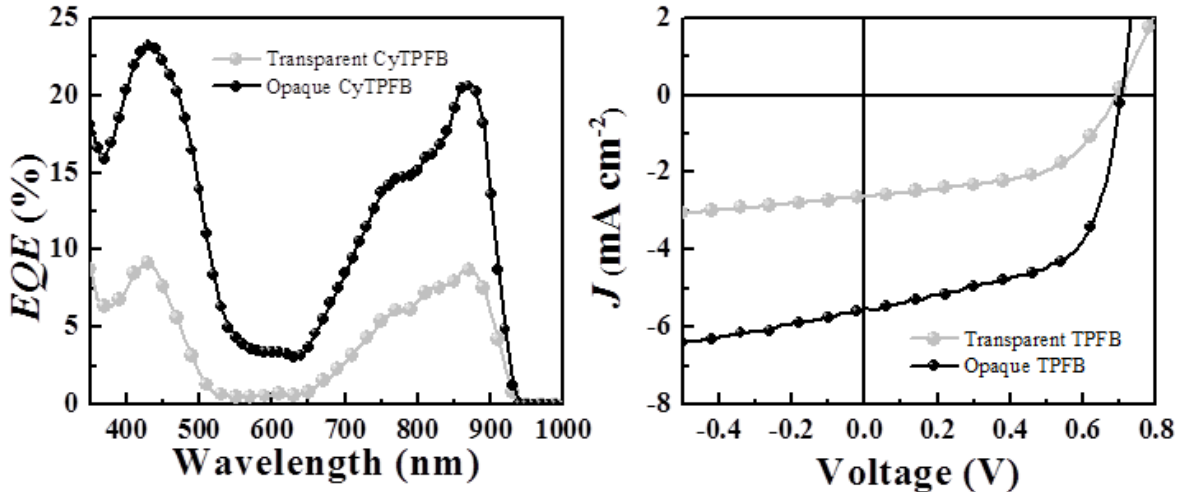

Figure S4. *J-V* and *EQE* performance of the opaque and transparent CyTPFB devices. A peak *EQE* of 9% at 870 nm and a *PCE* of 0.95% was achieved for these preliminary devices.

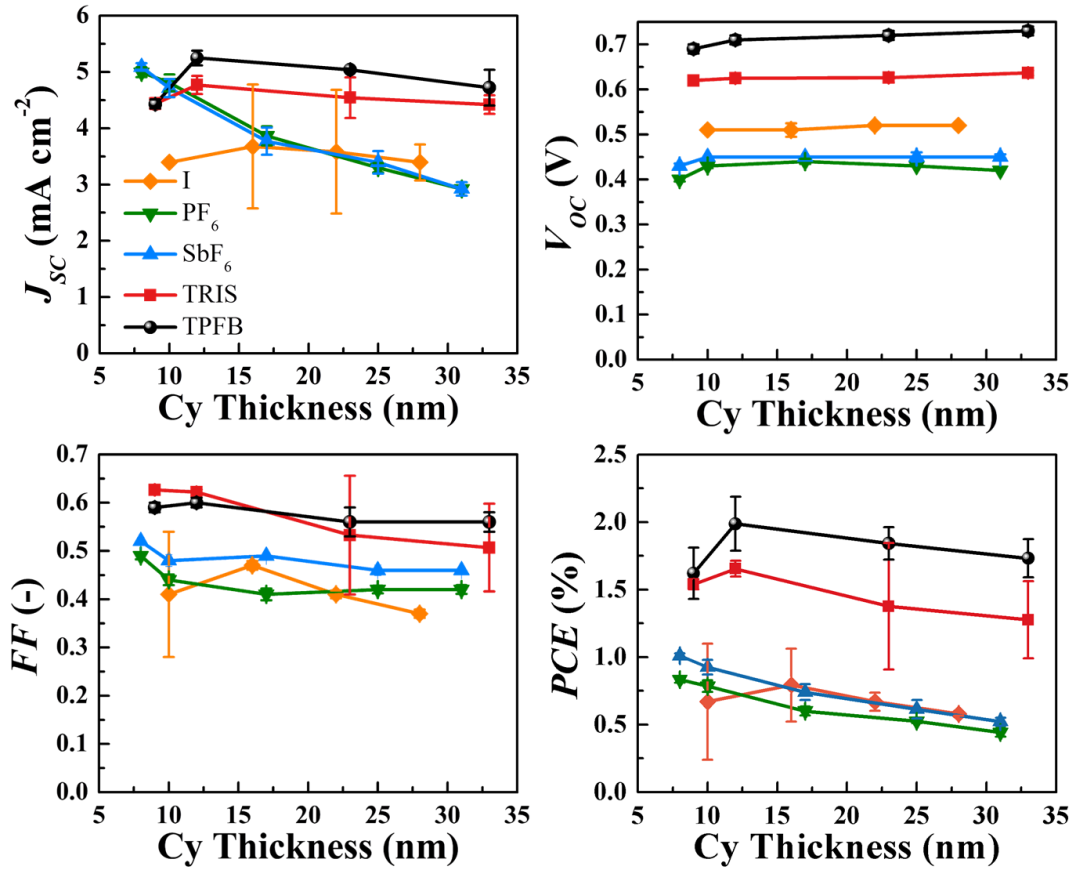

Figure S5. Thickness dependent *J-V* characteristics for each counterion. CyTRIS and CyTPFB show significantly less J_{SC} roll-off than the other counterions, which provides additional support for the increase in the fitted exciton diffusion lengths.

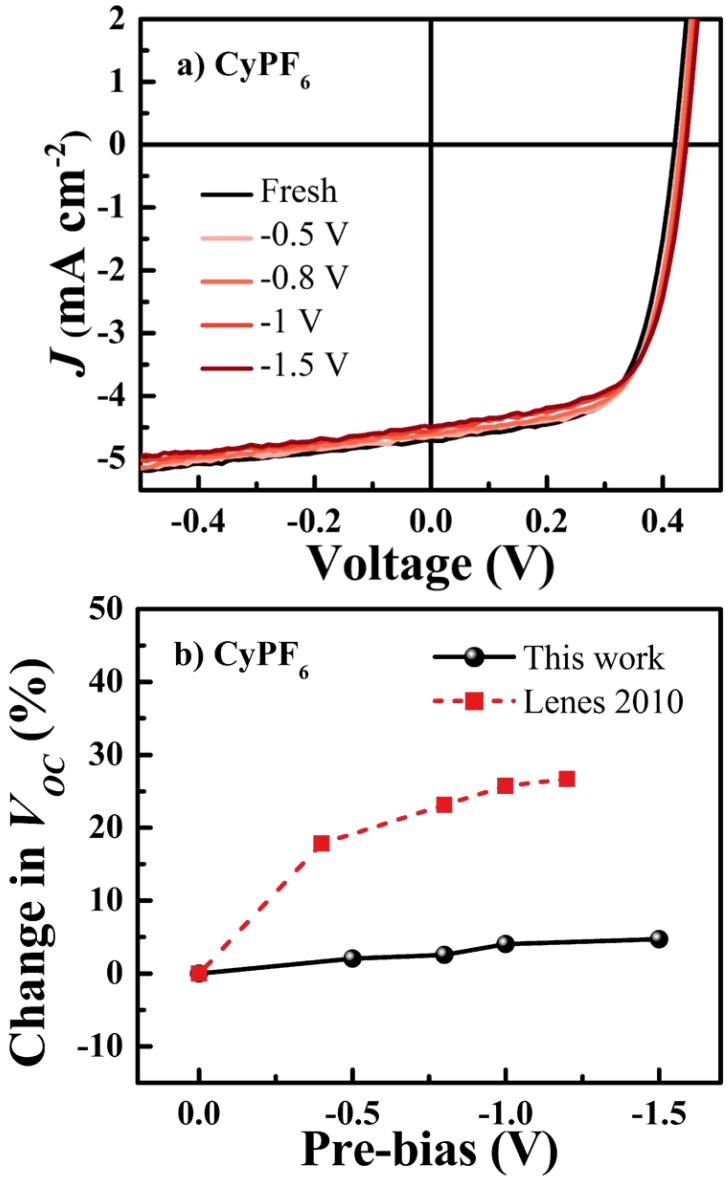

Figure S6. (a) *J-V* curves for $CyPF_6$ devices pre-biased for >10 min at 0 (Fresh), -0.5, -0.8, -1, and -1.5 V. Pre-biasing was performed in air on the same device sequentially from -0.5 V to -1.5 V, with ~1 min pauses to acquire *J-V* curves. V_{OC} shows a negligible variation after holding the device under negative bias for over 40 min. (b) Comparison between pre-biasing influence on V_{OC} in this work and in a previous study on a smaller, visible polymethine cation with PF_6^- and ClO_4^- as anions.[10]

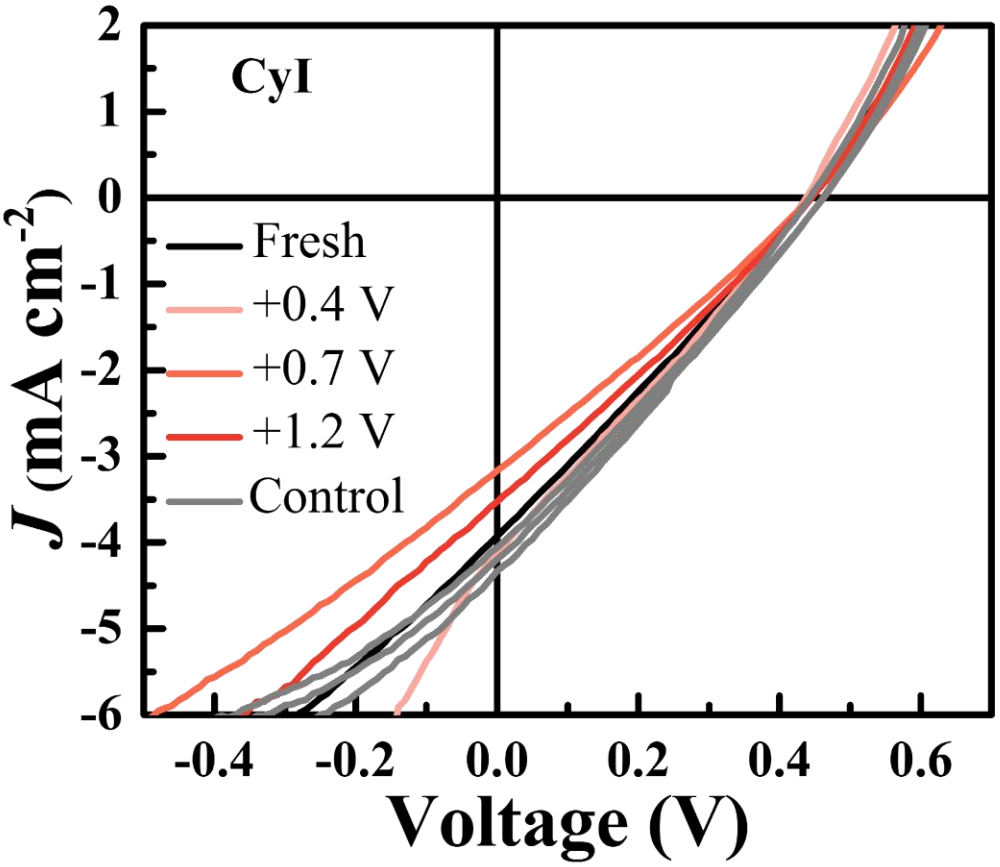

Figure S7. *J-V* curves for CyI devices under positive bias for >10 min at each voltage step. No significant effect on V_{OC} is observed, but J_{SC} changes by ~10% and does not decrease monotonically with increasing pre-bias voltage. Controls are plotted in grey and were taken concurrently with the biased device after each pre-biasing step. Again, these results do not show nearly as strong an effect as seen previously,[10] and suggest that ion diffusion does not play a significant role in these devices.

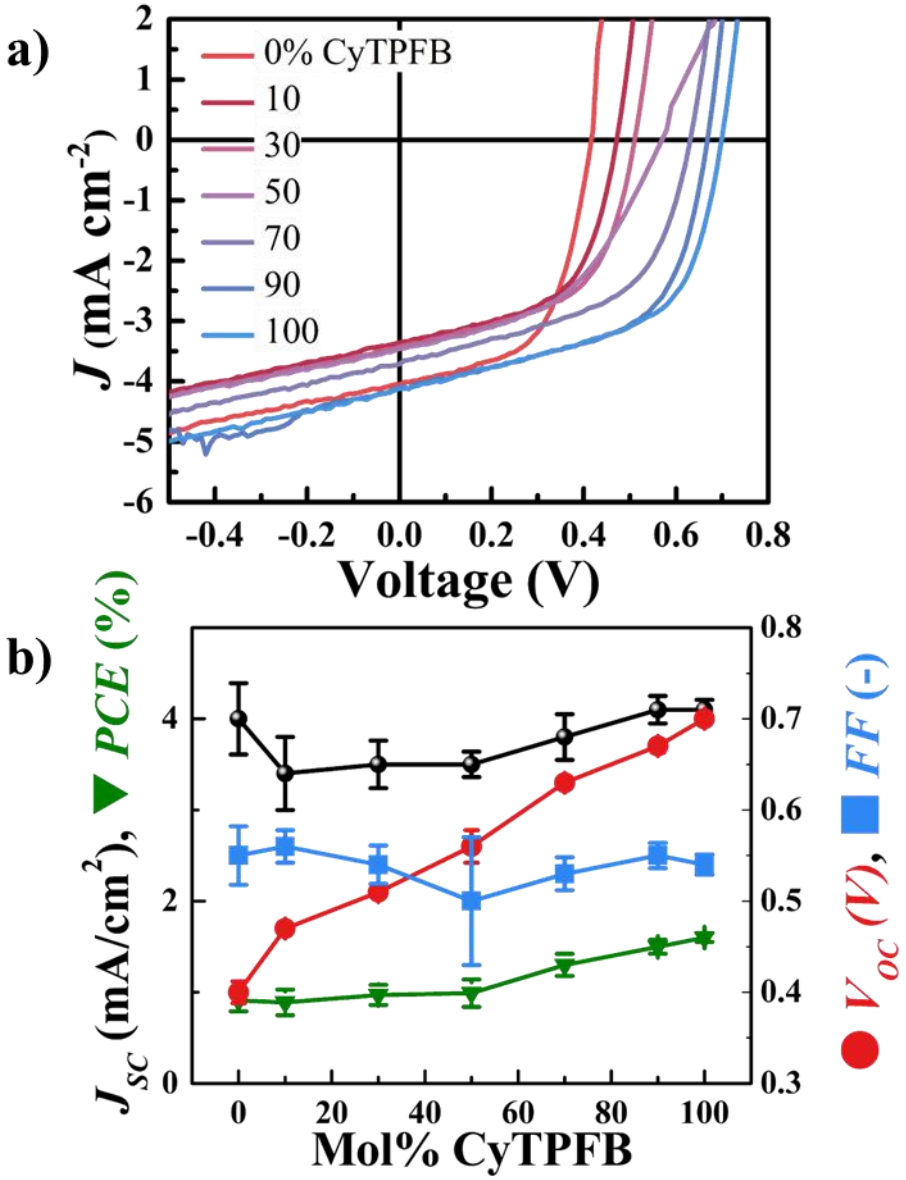

Figure S8. (a) *J-V* curves the $CyPF_6$ and CyTPFB mixing experiment. (b) Summary of the *J-V* parameters as a function of mol.% CyTPFB.

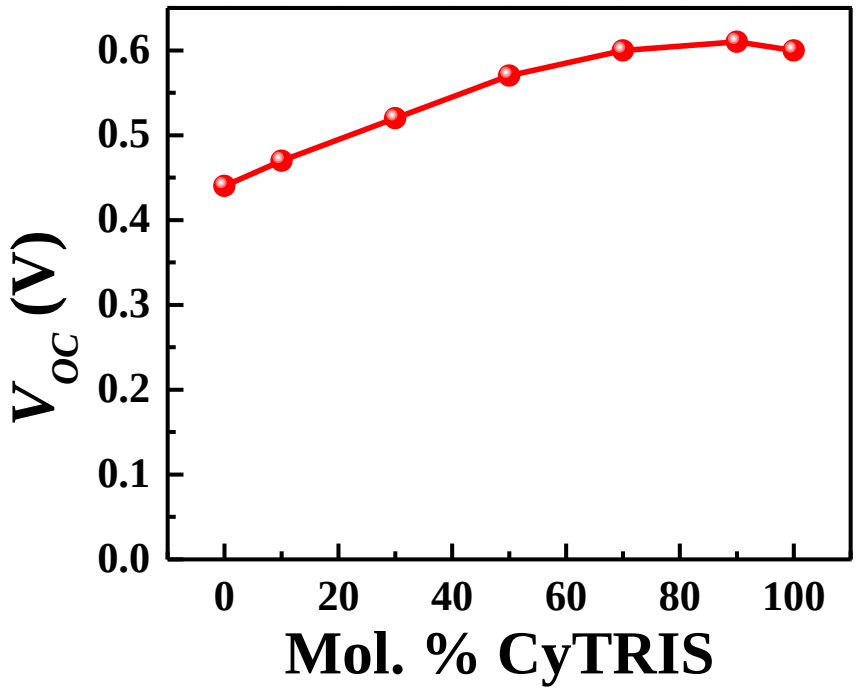

Figure S9. V_{OC} values for mixing between $CySbF_6$ and CyTRIS. A similar linear averaging trend is seen, as in the $CyPF_6$ – CyTPFB case highlighted in Figure S8.

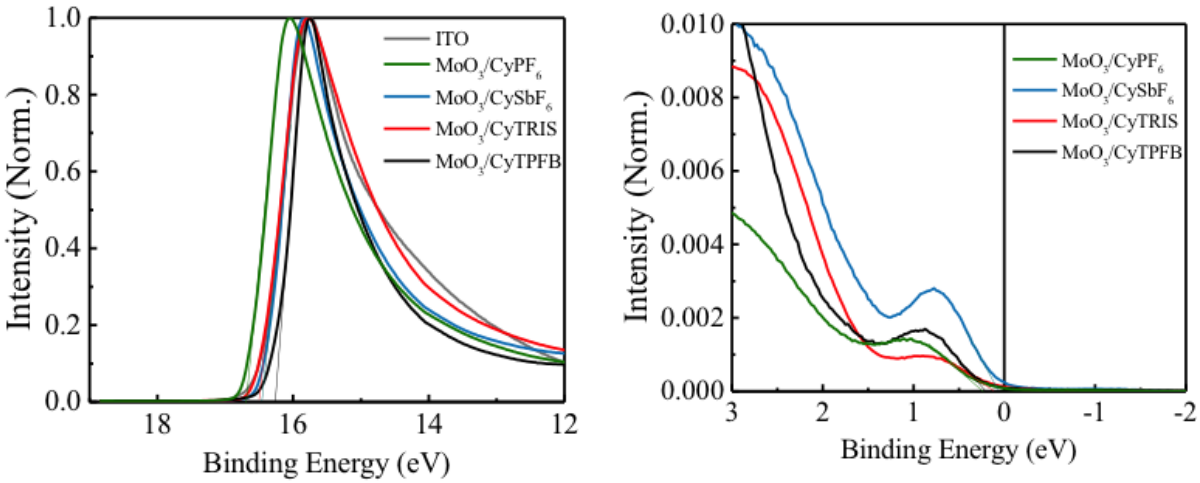

Figure S10. Ultraviolet Photoelectron Spectroscopy (UPS) data for ITO and each salt on ITO/MoO_3.

Table S1. Extracted parameters from UPS data: upper and lower energy cut-offs, work function, and HOMO levels. The HOMO level trend follows the observed V_{OC} enhancement in CyTRIS and CyTPFB devices.

Material	High Cutoff (eV)	Low Cutoff (eV)	Work Function	HOMO (eV)
ITO	16.40	0	4.80	-
$MoO_3/CyPF_6$	16.65	0.25	4.55	4.8
$MoO_3/CySbF_6$	16.45	0.05	4.75	4.8
MoO_3/CyTRIS	16.50	0.20	4.70	4.9
MoO_3/CyTPFB	16.25	0.25	4.95	5.2

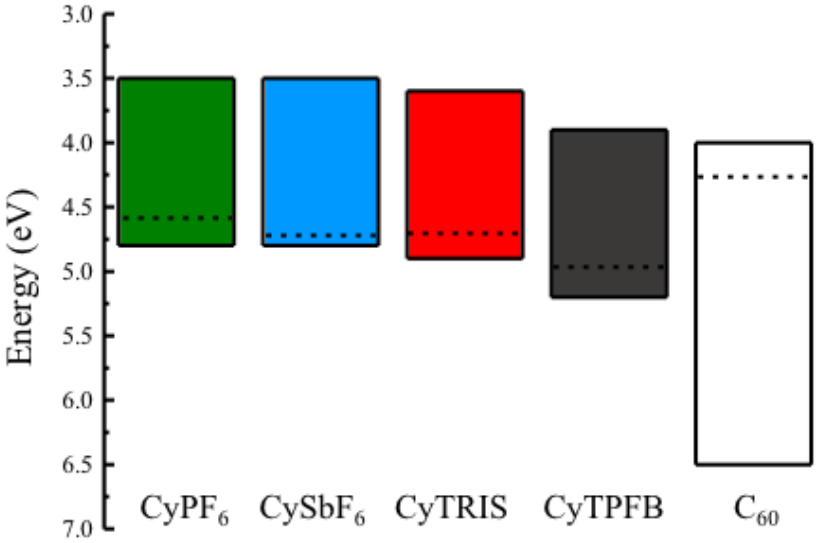

Figure S11. Energy level schematic measured for each anion. LUMO levels are approximated as the HOMO level plus the optical excitonic gap (~1.3 eV).

Table S2. Optical gaps, open-circuit voltages, and comparison to Shockley-Queisser (SQ) and realistic excitonic (Exc.) voltage limits for state-of-the-art organic salt photovoltaics.

Counterion	$\Delta\lambda_g$ [nm]	E_g^{opt} [eV]	V_{OC} [V]	% of SQ Limit	% of Exc. Limit	Notes	Ref.
I^-	953	1.30	0.45	43%	54%	–	This work
I^-	700	1.77	0.54	36%	45%	DSSC	[1]
I^-	623	1.99	0.63	37%	47%	Polymer	[2]
ClO_4^-	685	1.81	0.66	44%	54%	–	[3]
ClO_4^-	685	1.81	0.74	43%	54%	Space charge effects	[3]
ClO_4^-	665	1.86	0.79	49%	61%	–	[4]
ClO_4^-	635	1.95	0.72	50%	63%	Oxidative Doping	[5]
PF_6^-	945	1.31	0.4	38%	47%	–	This work
PF_6^-	918	1.35	0.38	35%	43%	–	[6]
PF_6^-	750	1.65	0.62	45%	56%	–	[4]
PF_6^-	665	1.86	0.79	50%	63%	–	[4]
PF_6^-	660	1.88	0.65	41%	51%	–	[3]
PF_6^-	630	1.97	0.72	43%	54%	PANI interlayer	[7]
PF_6^-	630	1.97	0.86	52%	64%	Inverted	[8]
PF_6^-	621	2	1	59%	74%	Meniscus Coating	[9]
PF_6^-	621	2	0.92	54%	68%	–	[4]
PF_6^-	615	2.02	0.56	33%	41%	–	[10]
PF_6^-	600	2.07	0.92	52%	65%	–	[11]
SbF_6^-	945	1.31	0.45	43%	53%	–	This work
Δ-$TRIS^-$	927	1.34	0.62	57%	72%	–	This work
Δ-$TRIS^-$	893	1.39	0.63	56%	70%	–	[6]
$TPFB^-$	927	1.34	0.71	66%	82%	–	This work

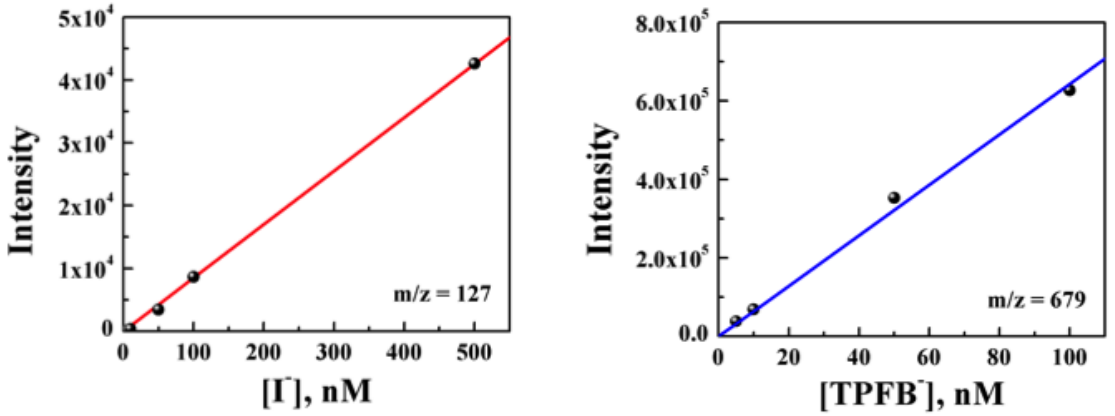

Figure S12. Standard reference curves for I^- and $TPFB^-$. The base solutions of CyI and K-TPFB, respectively, were both dissolved in acetonitrile.

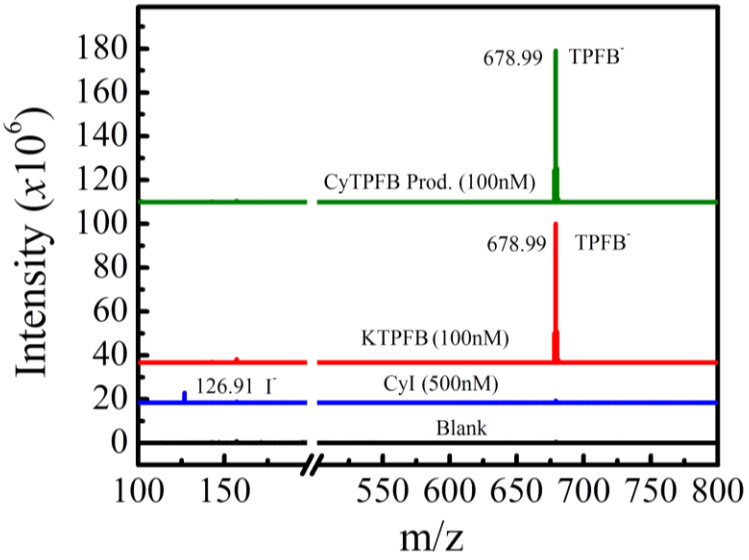

Figure S13. Mass spectra for the blank, reference solutions, and CyTPFB product.

Table S3. Measured concentrations of each anion in the CyTPFB product. Measured concentrations are calculated by comparing peak intensities with the standard reference curves, and any difference in the prepared and measured concentrations are likely due differences in the analyte response factors of KTPFB (the reference solution) and CyTPFB (the analyte).

CyTPFB concentration, nM	$[TPFB^-]$	$[I^-]$
5	7 ± 1	< 1
10	12 ± 1	< 1
50	60 ± 2	< 1
500	106 ± 1	< 1

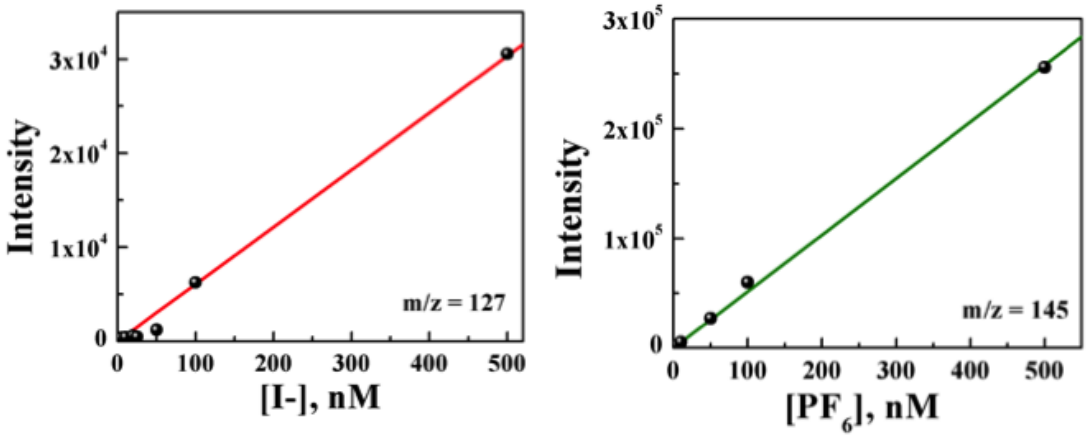

Figure S14. Standard reference curves for I^- and PF_6^-. The base solutions of CyI and $NaPF_6$ were dissolved in 50%/50% ACN/H_2O.

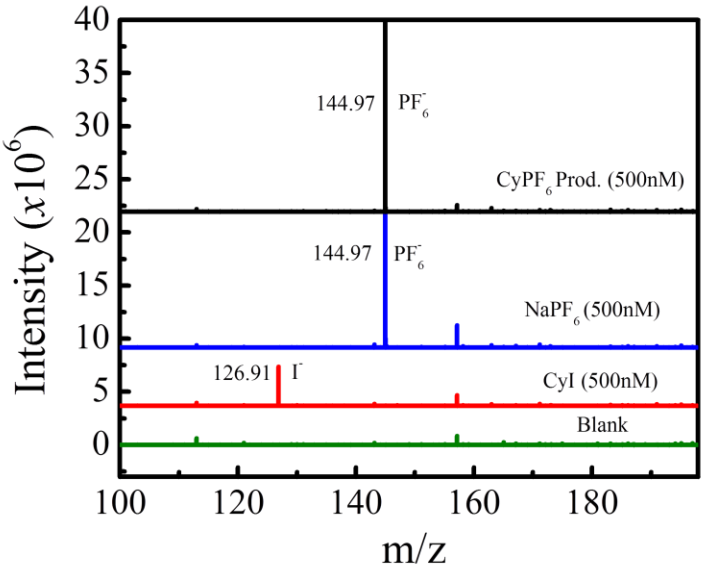

Figure S15. Mass spectra for the blank, reference solutions, and $CyPF_6$ product.

Table S4. Measured concentrations of each anion in the $CyPF_6$ product. Measured concentrations are calculated by comparing peak intensities with the standard reference curves, and any difference in the prepared and measured concentrations are likely due differences in the analyte response factors of $NaPF_6$ (the reference solution) and $CyPF_6$ (the analyte).

$CyPF_6$ concentration, nM	$[PF_6^-]$	$[I^-]$
5	2.9	5.9
10	5.1	4.1
50	38	4.1
100	65	3.5
500	333	3.9

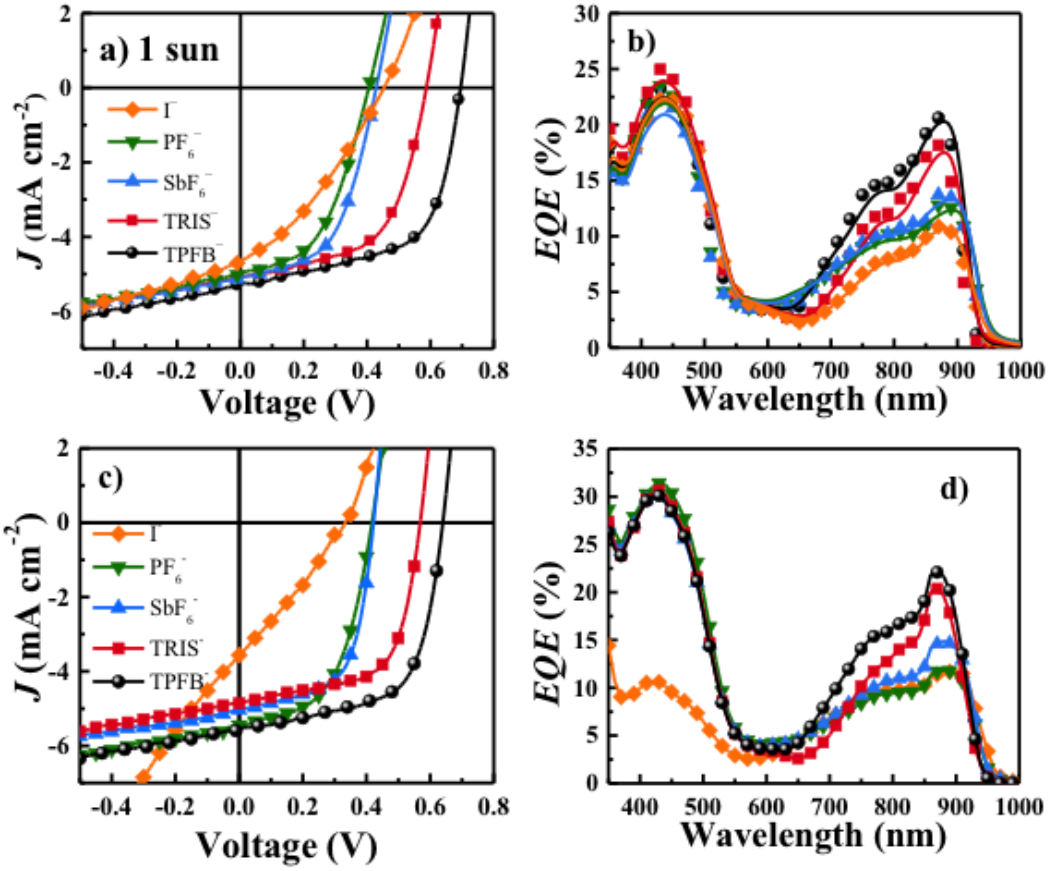

Figure S16. Influence of solvent on *J-V* and *EQE* parameters: in (a) and (b), data shown are from the paper using devices spin coated from chlorobenzene (CB) solutions for CyI, $CyPF_6$, $CySbF_6$, and CyTRIS, and a 3:1 CB:dichloromethane (DCM) solution. In (c) and (d) the donor layers are all spin coated from a 3:1 CB:DCM solution. It is clear that the solvent has no effect on the *J-V* parameters, nor any clear effect on *EQE*, except in the case of CyI. It is likely that the poor performance of CyI in this case is due to an outlier device set, and not a real effect from the change of solvent.

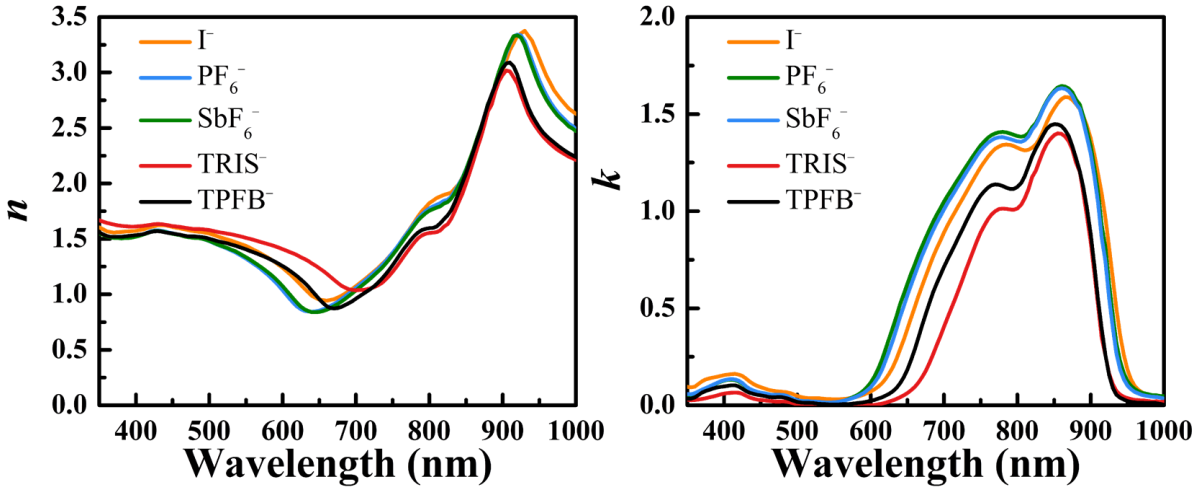

Figure S17. Real (*n*) and imaginary (*k*) indices of refraction for each counterion (left and right, respectively), as determined by variable angle ellipsometry. The *k* for CyTPFB and CyTRIS are slightly

lowered compared to the other counterions, most likely due to an optical spacing (density) effect. The peak widths for CyTPFB and CyTRIS are also reduced, likely due to decreased polarization and bond length alternation of the cation.[12]

References

[1] W. Wu, J. Hua, Y. Jin, W. Zhan, H. Tian, *Photochem Photobiol Sci* **2008**, *7*, 63.
[2] L. Wang, C. Hinderling, S. Jenatsch, F. Nüesch, D. Rentsch, R. Steim, H. Zhang, R. Hany, *Polymer* **2014**, *55*, 3195.
[3] M. Lenes, H. J. Bolink, *ACS Appl. Mater. Interfaces* **2010**, *2*, 3664.
[4] O. Malinkiewicz, T. Grancha, A. Molina-Ontoria, A. Soriano, H. Brine, H. J. Bolink, *Adv. Energy Mater.* **2013**, *3*, 472.
[5] B. Fan, F. A. de Castro, J. Heier, R. Hany, F. Nüesch, *Org. Electron.* **2010**, *11*, 583.
[6] A. C. Véron, H. Zhang, A. Linden, F. Nüesch, J. Heier, R. Hany, T. Geiger, *Org. Lett.* **2014**, *16*, 1044.
[7] B. Fan, F. Araujo de Castro, B. T.-T. Chu, J. Heier, D. Opris, R. Hany, F. Nüesch, *J. Mater. Chem.* **2010**, *20*, 2952.
[8] E. Berner, T. Jäger, T. Lanz, F. Nüesch, J.-N. Tisserant, G. Wicht, H. Zhang, R. Hany, *Appl. Phys. Lett.* **2013**, *102*, 183903.
[9] O. Malinkiewicz, M. Lenes, H. Brine, H. J. Bolink, *RSC Adv.* **2012**, *2*, 3335.
[10] R. Hany, B. Fan, F. A. de Castro, J. Heier, W. Kylberg, F. Nüesch, *Prog. Photovolt. Res. Appl.* **2011**, *19*, 851.
[11] G. Wicht, S. Bücheler, M. Dietrich, T. Jäger, F. Nüesch, T. Offermans, J.-N. Tisserant, L. Wang, H. Zhang, R. Hany, *Sol. Energy Mater. Sol. Cells* **2013**, *117*, 585.
[12] P.-A. Bouit, C. Aronica, L. Toupet, B. Le Guennic, C. Andraud, O. Maury, *J. Am. Chem. Soc.* **2010**, *132*, 4328.